Title: Improving Air Leakage Prediction of Buildings using the Fan Pressurization Method with the Weighted Line of Organic Correlation

Authors: Benedikt Kölsch[1] (corresponding author)

Iain S. Walker, PhD[2]

Affiliations:

1. Institute of Solar Research
   German Aerospace Center (DLR)
   Karl-Heinz-Beckurts-Str. 13
   52428 Jülich, Germany
   Email: benedikt.koelsch@dlr.de
   Phone: +49 2203 601 2707
   Fax: +49 2203 601 4170

2. Building Technology and Urban Systems Division
   Lawrence Berkeley National Laboratory
   1 Cyclotron Road
   Berkeley, CA 94720, USA

Improving Air Leakage Prediction of Buildings using the Fan Pressurization Method with the Weighted Line of Organic Correlation

ABSTRACT

In many countries, the fan pressurization method is the most frequently chosen approach for measuring the air leakage of houses. The measurements are usually performed at pressures that far exceed pressures to which buildings are exposed to under normal conditions. A fit of these tests to the power-law formulation allows an extrapolation to data points outside the measured pressure range. With the Ordinary Least Square (OLS) fitting method, the pressure exponent and flow coefficient can be determined. However, the measurement results are highly sensitive to uncertainties induced by external factors like changing wind conditions during the tests, which is neglected by OLS. This may lead to errors in the prediction of flows at lower pressures. The Weighted Line of Organic Correlation (WLOC) is an alternative approach and takes measurement uncertainty into account.

In this paper, a statistical analysis of an extensive data set of pressurization measurements has been performed. Both regression techniques have been compared for almost 7500 fan pressurization measurements of six houses in 109 different house leak configurations. The variability in predicting pressure exponent and flow coefficient for both WLOC and OLS regression was analyzed using probability density functions. It was found that the Weighted Line of Organic Correlation significantly decreases the uncertainty in predicting pressure exponent, flow coefficient, and other low-pressure air leakage metrics compared to the Ordinary Least Square fitting. The authors highly recommend the implementation of WLOC in current

measurement standards and test equipment.

Keywords

Fan Pressurization, Weighted Line of Organic Correlation, Ordinary Least Square Fitting, Power Law, Building Envelope, Airtightness

1. INTRODUCTION

According to the International Energy Agency [1], the residential and non-residential buildings together accounted for 30 % of the global final energy use and 28 % of energy-related CO_2 emissions in 2018. In addition to the industry (32 %) and the transport sector (28 %), buildings are, therefore, a key to the viability of current climate goals. Globally, space heating is the primary source of energy consumption in the building sector, and space cooling is one of the fastest-growing sources. The uncontrolled airflow through the building envelope contributes significantly to this increased consumption of heating and cooling energy [2–4]. In addition to rising costs for homeowners and higher greenhouse gas emissions, this can lead to an impairment of indoor air quality [5], can significantly affect the performance of existing ventilation systems [6] or may cause construction damages through mold formation inside walls [7,8].

The airtightness of building envelopes is typically ascertained by the fan pressurization method ("blower-door test"), which is specified in various standards like ASTM E779 [9], DIN EN ISO 9972 [10] or CAN/CGSB 149.10 [11]. A pressure difference is applied across the building envelope with a fan, which moves air in (pressurization) and out (depressurization) of a building. Typically, the airflow through the fan is determined by the pressure difference across a previously calibrated orifice. The pressure difference and the respective airflow through the fan

are recorded at several pressure differences.

The pressure range across the envelope during the measurements dramatically exceeds the pressures leaks in a building are exposed to under normal operation. At these higher pressure differences, relative impacts due to ambient disturbances (like wind) and uncertainty of the measurement devices are usually lower. However, a subsequent interpolation of the measured pressures and an extrapolation to low pressure where natural infiltration occurs may contain a significant uncertainty [12]. Therefore, the most precise measurements at high pressure are the least accurate ones [13,14]. The determination of infiltration at low pressures (< 4 Pa) may not be interesting to fulfill energy performance standards (e.g., passive house) or used in building standards to compare the relative airtightness of different buildings, but is essential for building energy calculations [15] or indoor air quality assessments [16]. Although measurement uncertainties may significantly influence the prediction of airflow rates at low pressures, the current standards do not necessitate the acquisition of uncertainties of the measured values.

The importance of the consideration of uncertainties in fan pressurization measurement was already discussed by Persily et al. [17] in 1985 and Herrlin et al. in 1988 [18]. Geissler performed simulations about the estimation of errors of blower door measurements [19]. Sherman et al. [20] analyzed in 1995 the errors of extrapolation to low pressures using the Ordinary Least Square (OLS) regression method. Recent studies also confirmed that the uncertainty of fan pressurization measurements could not be neglected [21]. Furthermore, Carrié et al. [22] recently highlighted, in particular, the influence of wind fluctuations and frequency on the uncertainty of building airtightness pressurization tests.

In addition to the conventionally used OLS regression method, Delmotte et al. [23] discussed in 2011 the applicability of a weighted least square regression, and Okuyama et al. [24] introduced

in 2012 an Iterative Weighted Least Square (IWLS) regression approach. In 2017, Delmotte [25] suggested the Weighted Line of Organic Correlation (WLOC) as an improved non-iterative regressing method, which takes measurement uncertainties into account.

In this work, the OLS and WLOC regression methods are applied to a large dataset of almost 7500 blower-door measurements in six different single-story, single-family houses. The goal was to identify the uncertainties in the prediction of the pressure exponent and flow coefficient of the power-law using both regression techniques. In addition to the work done by Prignon et al. [26,27], this work investigates a statistical analysis of a larger data set of blower door measurements.

2. METHODOLOGY

2.1. Test Site and Measurement Equipment

In this paper, a data set of fan pressurization measurements is used, which was recorded at the Alberta Home Research Facility (AHHRF). This facility consists of six unoccupied houses, which are each of different construction. These houses were located south of Edmonton, Alberta, Canada, and were used to test different heating and ventilation strategies. Each of these six houses is a single-story construction with a floor area of 6.7 m by 7.3 m, a wall height of 2.4 m, and a full basement. For more detailed information about this test facility and data source, see [14] and [28].

Repeated fan pressurization measurements have been performed at each of these six houses. These repetitions allow an investigation of how external factors (like the presence and strength of wind) may affect the measurement results when the building construction and, therefore, the airtightness remain constant. All tests were automated, which prevents additional uncertainties

due to equipment installation and operator errors, and enables the recording of a large data set. A total of almost 7500 fan pressurization tests have been performed, where each test contains between 20 and 100 measurements of pressure difference and airflow rate, which enables to obtain a complete flow-pressure difference characteristic for each test. The covered pressure range lies between 1 and 100 Pa, for both pressurization and depressurization, which is a broader range than required by the ASTM E779 [9] or DIN EN ISO 9972 [10] standard.

The houses were operated in 109 different test configurations, e.g., pressurization and depressurization tests, open and closed flues, windows, or passive vents. Prior to this analysis, the data set was filtered to remove erroneous files, where, e.g., no standard deviation or offset pressure was recorded. This filtering results in 7402 sets of measurements from the original 7500 sets being selected for this study.

Because wind (and stack) pressures vary over the building envelope, the testing procedure would ideally measure the indoor-outdoor pressure difference at each leak location. However, this approach is impractical. For this study, indoor-outdoor pressure differences were taken from pressure taps on each wall of the test building connected to a pressure averaging manifold. This averaging of multiple pressure taps was intended to reduce uncertainties and biases due to wind speed and direction [29] and follows the guidance in standardized testing [9]. Despite the use of multiple pressure taps, we still expect some test uncertainty due to varying wind direction during a test. Wind direction was measured during these tests, but the additional analysis of wind direction effects is beyond the scope of this paper, and we note that wind direction effects will also scale with wind speed, with the effect of wind direction variability being more significant at higher wind speeds.

In most field measurements, only one pressure tap is used to record outside pressure data and

may result in higher sensitivities than presented here. Each measured envelope pressure consisted of about 150 individual measurements over a period of 15 seconds. The mean and standard deviations of the pressure measurements at each station are recorded. These standard deviations are used as an uncertainty estimate for each pressure station and are an essential input to the WLOC analysis.

In contrast to the required measurement procedure in most standards, where offset pressures have to be recorded at the beginning and end of each measurement series, for this study, every pressure difference data point has been corrected by a reference pressure at zero flow rate for this point in this analysis. For this purpose, a damper closed the fan opening for each offset pressure measurement because this opening may affect the pressure distribution throughout the building.

The airflow rates Q (in m³/h) were measured using a laminar element flowmeter, which was connected to the outside with a flexible duct. All flow rates were corrected with indoor and outdoor air temperatures according to the ASTM E779 [9] standard. As with the pressure difference measurements, the air flows were taken over a period of 15 seconds, at a sampling rate of about ten samples per second. From the pressure measurements across the laminar element flowmeter, both the mean $\Delta P_{flowmeter}$ (in Pa) and standard deviation ($\sigma_{\Delta P\ flowmeter}$) were recorded. Due to the linear behavior of the flowmeter, the respective standard deviation of the airflow (σ_Q) was determined by the following equation:

$$\sigma_Q = \sigma_{\Delta P\ flowmeter} \cdot \frac{Q}{\Delta P_{flowmeter}} \qquad (1)$$

In this data set, a wide range of weather conditions are covered with outside temperatures between –40°C and +30°C and wind speeds of up to 10 m/s. The wind speed, wind direction, and ambient temperature data were gathered from a meteorological station next to the test site.

2.2. Regression Methods

In the past, there were several approaches [30–32] to predict the relationship between the airflow rate Q and the pressure difference ΔP (in Pa) across the building envelope. The current formulation in all measurement standards is the power-law relationship [33]:

$$Q = C\Delta P^n \quad (2)$$

C (in $m^3/(h \cdot Pa^n)$) is the flow coefficient, which can be a measure of the overall leakage size, and n is the pressure exponent, which characterizes the leakage shape [34]. The flow exponent is limited to values between 0.5 (turbulent flow) and 1.0 (laminar flow) but is typically in the vicinity of 2/3 [33]. This formulation is a reasonable model to describe the airflow through a network of cracks that can vary in size and shape in a building envelope.

For the determination of flow coefficient and pressure exponent, this power-law needs to be transformed to its linear form by expressing both sides of Eq. (2) for each measured value as logarithms:

$$\ln(Q) = \ln(C) + n \cdot \ln(\Delta P) \quad (3)$$

A regression is applied to this linear form of the power law, where n is the slope, and $\ln(C)$ is the intercept of this regression. In the following paragraphs, the OLS and the WLOC regression techniques, which are compared in this study, are introduced.

2.2.1. Ordinary Least Square Method

In current standards [9, 10], the Ordinary Least Square (OLS) method is used for determining the flow coefficient C and pressure exponent n. The OLS method minimizes the residuals, which are geometrically the distances in the y-direction between the fitted line and the measured values [35]. In this case, $x_i = \ln(\Delta P_i)$ is the independent and $y_i = \ln(Q_i)$ is the dependent variable

(with $1 \leq i \leq N$). The pressure exponent and flow coefficient of the power-law formulation (cf. Eq. (2)) can directly be determined using following formulas:

$$n = \frac{\sum_{i=1}^{N}\left(x_i - \sum_{i=1}^{N}\frac{x_i}{N}\right)\left(y_i - \sum_{i=1}^{N}\frac{y_i}{N}\right)}{\sum_{i=1}^{N}\left(x_i - \sum_{i=1}^{N}\frac{x_i}{N}\right)^2} \quad (4)$$

$$C = exp\left(\sum_{i=1}^{N}\frac{y_i}{N} - n \cdot \sum_{i=1}^{N}\frac{x_i}{N}\right) \quad (5)$$

Here, the assumption is made that values in the y-direction are equally uncertain, and the uncertainties in the x-direction, which correspond to the pressure difference measurements, are not taken into account [36]. These assumptions are, however, not valid for measurements in real buildings. Imperfect knowledge of the uncertainties may lead to a shifting and rotation of the linear regression line of the power-law. The fractional error is usually more significant for lower pressure points (e.g., 4 or 10 Pa) than for higher pressure points and may lead, therefore, to uncertain predictions of flows at these pressures [25].

2.2.2. Weighted Line of Organic Correlation

In contrast to OLS, the Weighted Line of Organic Correlation (WLOC) minimizes the sum of the product of the measured values and the weighted horizontal as well as vertical differences and the predicted line [25]. Consequently, measurement points with higher uncertainty are less significant in the calculation of the regression line. This is an important characteristic, mainly if airflows at low pressures shall be predicted. Unlike the Iterative Weighted Least Square (IWLS) regression approach [24], pressure exponent and flow coefficient can be calculated without iteration:

$$n = \frac{\sqrt{\sum_{i=1}^{N} v_i w_i \sum_{i=1}^{N} v_i w_i y_i^2 - (\sum_{i=1}^{N} v_i w_i \, y_i)^2}}{\sqrt{\sum_{i=1}^{N} v_i w_i \sum_{i=1}^{N} v_i w_i x_i^2 - (\sum_{i=1}^{N} v_i w_i \, x_i)^2}} \tag{6}$$

$$C = \exp\left(\frac{\sum_{i=1}^{N} v_i w_i \, y_i - n \cdot \sum_{i=1}^{N} v_i w_i \, x_i}{\sum_{i=1}^{N} v_i w_i}\right) \tag{7}$$

In Eq. (6) and (7), v_i and w_i are the weights of each measurement point x_i and y_i. These weights are defined by Delmotte [25] as the reciprocal value of the measured standard deviation at each pressure level:

$$v_i = \frac{1}{\sigma(x_i)} \tag{8}$$

$$w_i = \frac{1}{\sigma(y_i)} \tag{9}$$

Thus, lower variability in the measured data gives it more significant weight in the analysis, and therefore, these points are more important in the fitting.

In Figure 1, an example of a typical blower-door measurement with twelve different pressure differences and their corresponding airflow rates is shown. This specific example is just one out of the 7402 considered measurement series in this work in order to demonstrate the difference between the fitting of OLS and WLOC (a depressurization test of a masonry structure with an open 150 mm diameter furnace flue). The measured standard deviations for each point are displayed as well. For the same measurement series, both previously described regression methods are applied, and the resulting power-law functions are plotted on a linear scale. The Ordinary Least Square fitting (blue line) tries to find an appropriate fit for all pressure differences equally. In contrast, the Weighted Line of Organic Correlation (red line) considerably improves the fit for data points with low measurement uncertainty. Data with more significant

errors are less important in the fitting. In this specific case, WLOC shows a significantly better fitting for measurement data points in particular above 25 Pa pressure difference.

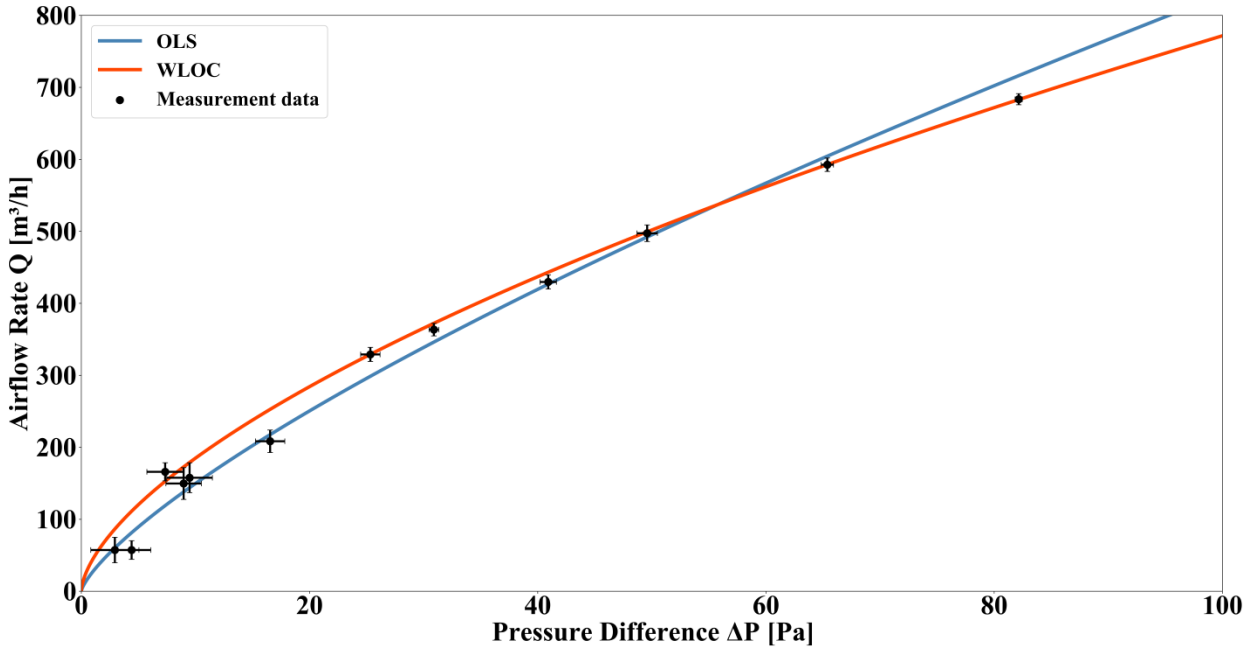

FIG. 1 Linear display of a comparison between OLS and WLOC fitting technique for one blower-door measurement series

2.3. Probability Density Functions

To determine the potential improvement using WLOC, we took the results for each of the 109 configurations and looked at the distribution of calculated *n* and *C* for both WLOC and OLS for multiple measurements. This comparison was achieved by the analysis of Probability Density Functions (PDFs) for each individual leakage configuration. The area under the PDF curve between two points equals the probability of getting a value between these two points. Therefore, not the value of the function is essential but the integral. Here, the PDFs were calculated using the Kernel Density Estimation (KDE) algorithm, which allows estimating an unknown

continuous density function from a set of N discrete 1D data samples $x_{s,i}$, with $1 \leq i \leq N$ [37]. The use of KDE has a significant advantage of directly evaluating the data without previously applying a model onto it [38]. In contrast to the commonly used histogram as an estimation of a datasets density, the shape of the kernel density estimation is continuous and seems to be a reasonable estimation of the "true" PDF [39]. According to Sheather [40], the bias of kernel density estimation is one order better compared to a histogram estimator.

The approximated PDF $\widehat{f_h}(x_s)$ was computed as (cf. [41]):

$$\widehat{f_h}(x_s) = \frac{1}{N \cdot h} \sum_{i=1}^{N} K\left(\frac{x_s - x_{s,i}}{h}\right) \tag{10}$$

Each observed sample is first replaced with a uniform kernel K, which is here based on the normal Gaussian distribution, which is the most frequently used kernel [39]:

$$K(x) = \frac{1}{\sqrt{2\pi}} e^{-\frac{x^2}{2}} \tag{11}$$

A summation of these curves and a subsequent normalization to obtain an area of 1 under the final curve, leads to an approximated PDF. The parameter h in Eq. (10) is the bandwidth, which adjusts the smoothness of the PDF and is calculated as recommended by Silverman [38]:

$$h = 1.06 \cdot \sigma \cdot N^{-\frac{1}{5}} \tag{12}$$

The narrower the distribution of the results (i.e., lower variance), the less sensitive the analysis is to experimental variation (primary from wind), and the lower the uncertainty is for any given test in predicting the correct leakage.

3. RESULTS AND DISCUSSION

Results are presented here in terms of PDFs of predictions of pressure exponent *n* and flow coefficient *C* for different leak configuration. We also examined the variability in other metrics that are commonly used: the building envelope flow and the equivalent leakage area at both 4 and 10 Pa reference pressures.

3.1. Pressure Exponent and Flow Coefficient

The PDFs were calculated for all 109 configurations. We provide example figures for illustration purposes. Each example is for one single leak configuration. The small vertical lines next to the x-Axis indicate the predicted values of *n* and *C* for a complete series of measurements using the OLS (blue line) and WLOC (red line) regression method, respectively. The global maximum of the PDFs can be interpreted as the mode and is here the expected true value of *n* and *C* for the respective data set and regression technique.

The results were broken down into five different fundamental cases:

1. **Equal expected values and higher variances for OLS:**

   In this case, both regression methods predict approximately the same values of *n* and *C*, but the PDFs of the OLS regression have a significantly higher variance. An example is shown in Figure 2. In this specific configuration, the OLS regression method predicts the pressure exponent values over a broad range, here between 0.55 and 0.78. The distribution of calculated pressure exponent values using the WLOC regression method is here limited between 0.57 and 0.69. Even though the highest density of calculated pressure exponents and flow coefficients for both regression methods has roughly the

same value ($n = 0.6$), the probability of getting close to this value with one single measurement, which is often done in field testing, is much higher using WLOC regression. For this specific configuration, the variance using the WLOC regressing technique is reduced by 67 % for the pressure exponent and by 52 % for the flow coefficient.

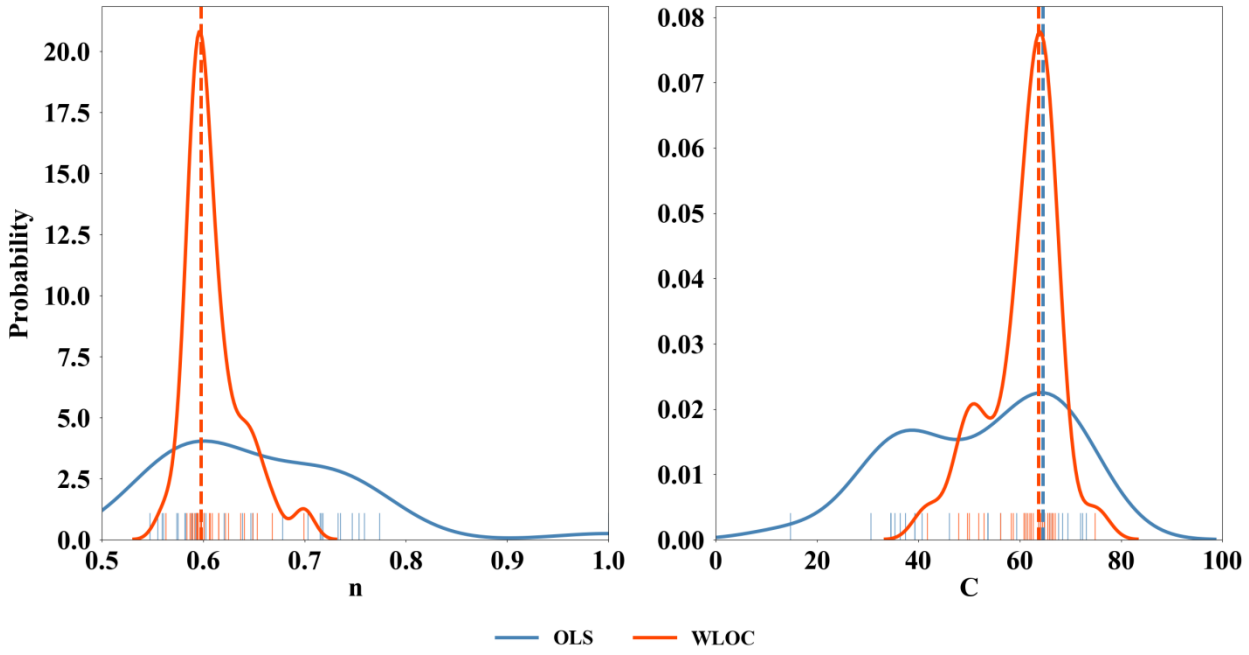

FIG. 2 PDF of calculation of *n* and *C* using OLS and WLOC fitting method, with a higher variance of OLS and approximately the same mean values

2. **Different expected values and higher variances for OLS:**

   The estimation of the expected values differs significantly for both regression techniques. In addition, the PDFs of the OLS regression method have a higher variance. Most of the investigated leak configurations fall into this case. In the displayed configuration (see Figure 3), the point of the highest density of the predicted pressure exponent *n* differs by

approximately 0.11 ($n_{OLS} = 0.76,\ n_{WLOC} = 0.65$). In most cases, a higher prediction of n simultaneously results in a lower prediction of C because C and n tend to be highly correlated [20]. The variance of n is reduced by 75 % and the variance of C by 61 % using WLOC in the displayed configuration. Thus, even with multiple fan pressurization measurement series, the probability of getting close to the correct values for n and C is challenging using OLS.

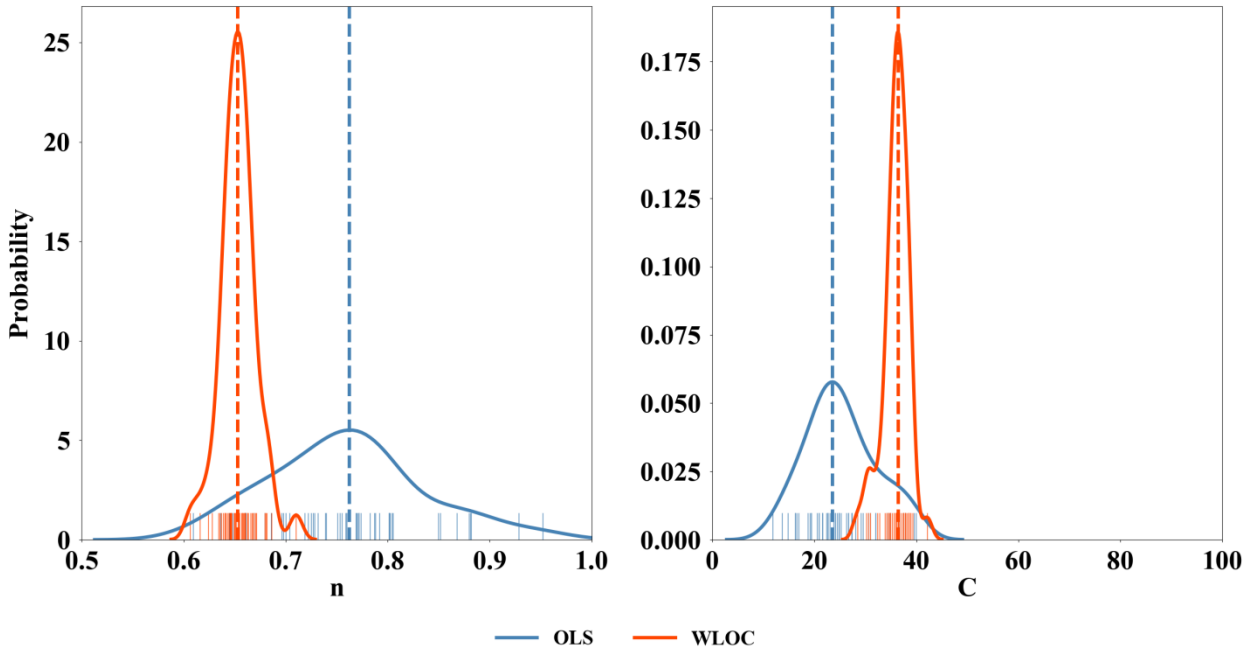

FIG. 3 PDF of calculation of n and C using OLS and WLOC fitting method, with a higher variance of OLS and different mean values

3. **Equal expected values and equal variances:**

In the third case, the shapes of the PDFs of pressure exponent and flow coefficient with both fitting methods are approximately the same. Here, both regression methods predict n and C with an equal probability. An example is shown in Figure 4, where $n = 0.67$ for both regression methods. In this case, the choice of regression method is of no

importance, because the performance of both is the same.

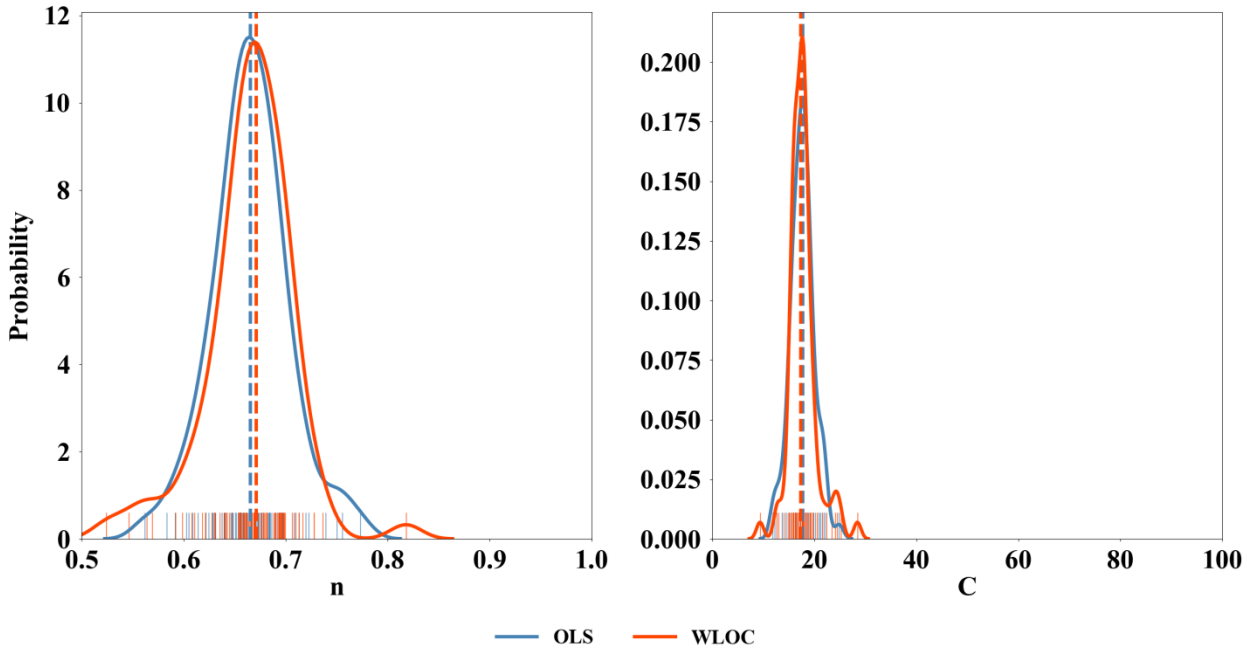

FIG. 4 PDF of calculation of n and C using OLS and WLOC fitting method, with approximately the same variances and the same mean values

4. **Different expected values and equal variances:**

The shapes of the PDFs classified as case 4 are similar and, therefore, the variances are similar for both regression techniques. However, the expected values are considerably different (see Figure 5, where $n_{OLS} = 0.66, n_{WLOC} = 0.61$). Here, it is not clearly evident which value of n or C can be interpreted as the true value for this configuration. Only a few leak configurations fall into this category.

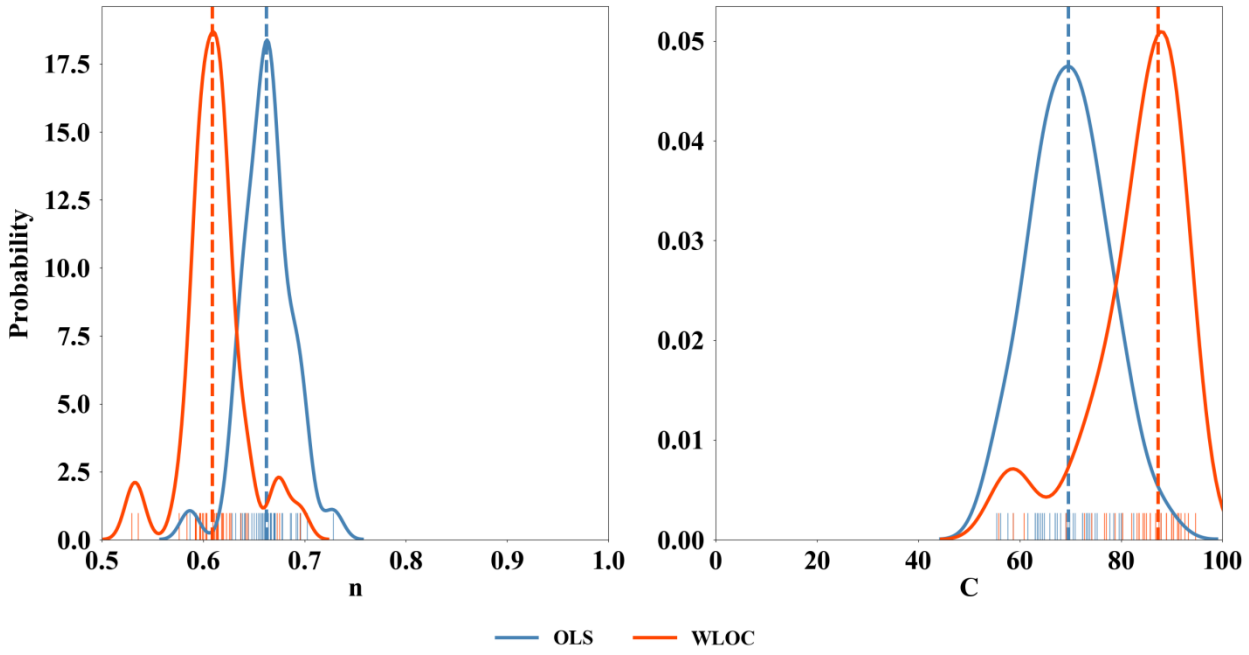

FIG. 5 PDF of calculation of *n* and *C* using OLS and WLOC fitting method, with approximately the same variances and different mean values

5. **Equal expected values and higher variances for WLOC:**

   This case is the opposite of case 1. Both regression methods predict values of *n* and *C*, which are very close to each other, but WLOC has a higher variance this time. In the example, displayed in Figure 6, the values for *n* are $n_{OLS} = 0.69$ and $n_{WLOC} = 0.70$. At leak configurations that fit in case 5, the WLOC regression method seems to perform worse than the OLS method. However, the number of configurations allocated to this case is far lower compared to the number of configurations in cases 1 or 2. Additionally, the number of measurements per leak configuration and thus, the number of data samples that were used to calculate the PDF was considerably lower for the configurations in case 5. Therefore, the reliability of these PDFs might be lower.

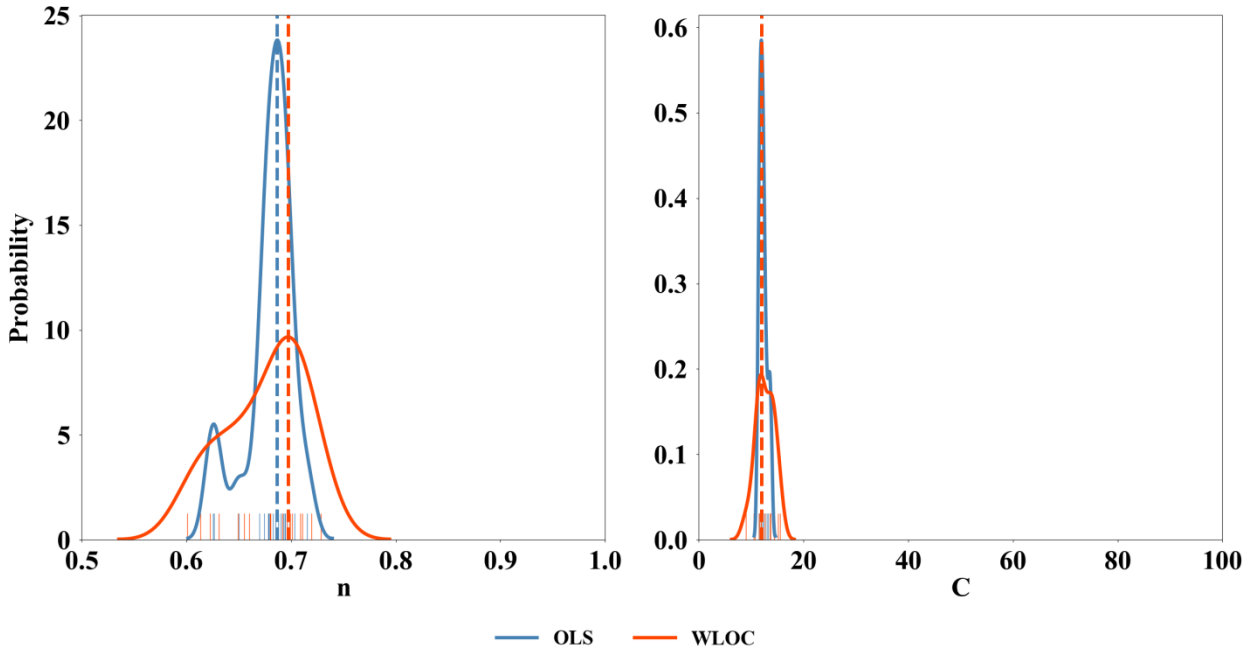

FIG. 6 PDF of calculation of *n* and *C* using OLS and WLOC fitting method, with a higher variance of WLOC and approximately the same mean values

There is no distinct case where the prediction of both regression curves is significantly different and where the variances of the PDFs of WLOC are higher.

The effectiveness of the WLOC approach depends on how often tests fall into these different categories. For this data set of 7.402 sets of measurements with 109 different test configurations, 17.4 % can be allocated to case 1, 40.5 % to case 2, 15.6 % to case 3, 7.3 % to case 4 and 12.8 % to case 5, which is shown in Figure 7. Only 6.4 % of the investigated tests cannot explicitly be allocated to one of these cases. The most popular case (case 2) has both a lower variance for WLOC and differences in predicted leakage parameters, *C* and *n*. This is an interesting result because we might have expected a lower variance for WLOC but not necessarily a change in the predicted value. Combining cases 2 and 4 shows that about half the tests show changes in predicted value between the two approaches. The example for case 5 shows that even when

WLOC has higher variance, it is not as high as the higher variance result for OLS. In most of the investigated leak configurations, the variance of WLOC is lower compared to OLS, and the expected value is different.

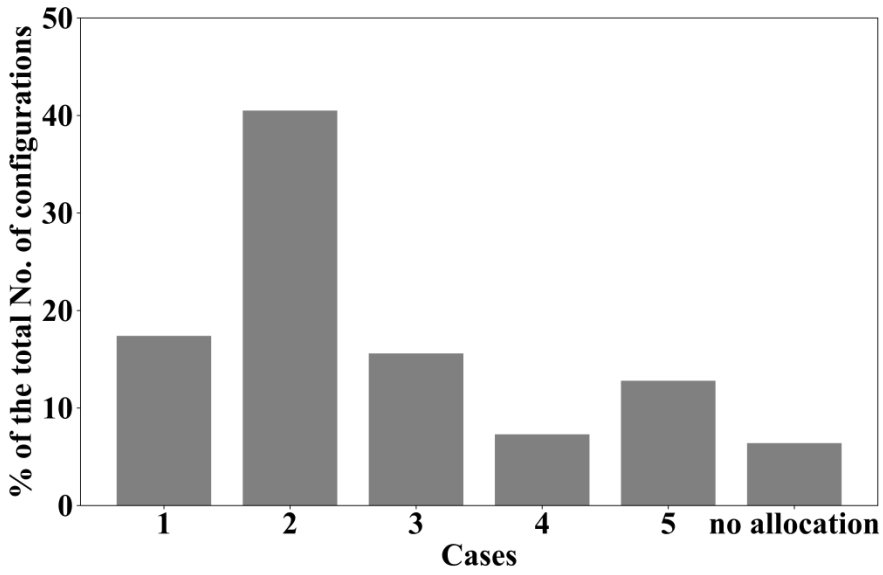

FIG. 7 Share of each case of the total number of investigated leak configurations

In 73.5 % of all investigated configurations, the WLOC regression technique that gives lower weighting to data with higher variability is better than or at least as good as the conventionally used OLS regression. Overall, the WLOC substantially reduces the variances in the test results on average for all 7402 tests by 32 % for pressure exponent *n* and by 22 % for flow coefficient *C*.

3.2. Airflow Rate and Equivalent Leakage Area

In addition to the test-to-test uncertainty, there may be biases introduced by testing at different wind speeds [29]. Here, the airflow rates and the equivalent leakage areas (ELAs) are shown for

one specific example (depressurization of a masonry structure with an open 150 mm diameter furnace flue). This example has been chosen because it contains a large amount of 65 tests.

The equivalent leakage area is the area of a sharp-edged hole (that has a pressure exponent of 0.5) that has the same flow at a fixed reference pressure as the power-law formulation. The ELA_4 at a pressure of 4 Pa can be defined as followed:

$$ELA_4 = \frac{Q_4}{C_D}\sqrt{\frac{\rho}{2\Delta P_4}} \tag{13}$$

Here, Q_4 (m^3/s) is the airflow at 4 Pa pressure difference, ρ (kg/m^3) is the density of air, C_D is a fixed discharge coefficient, and ΔP_4 is the reference pressure at 4 Pa.

To better observe the sensitivity of testing bias to wind, the results of the 65 repeated tests for this configuration were binned every 1 m/s of wind speed. This process reveals any biases due to testing at different wind speeds. The results are plotted as differences between the calculated value (using the power-law) and a reference value. This reference value has been chosen as the value with the lowest corresponding wind speed in the data set and can be seen as a benchmark to the other measurements at higher wind speeds because the influence of wind is the smallest. These reference cases at low wind speeds have also been used in previous studies, e.g., [14]. A good fit, and thus a reasonable estimation of airflow rates or ELAs at low pressures, is therefore characterized by a small difference between the estimated value and the reference value.

For this analysis, airflow rates and ELAs at 4 and 10 Pa pressure difference have been chosen. Airflow rates at 4 Pa pressure differences are relevant for users because it is a typical metric for energy simulations [15] or indoor air quality applications [16]. The ELA at 4 Pa pressure difference is part of the ASTM E779 standard [9] and is at 10 Pa pressure difference part of the Canadian CGSB 149.10 standard [11].

In Figure 8, the average relative airflow rate is plotted as a function of the mean wind speed during the measurement, evaluated at 4 (a) and 10 Pa (b) pressure difference. For mean wind speeds up to 2 m/s, both regression techniques appear to be equally good. For mean winds speed of more than 2 m/s, the difference between the reference value and the calculated values increases particularly for OLS up to 6 m/s. This increase in uncertainty at higher wind speeds has been recognized in the DIN EN ISO 9972 test method [10] that states that above a meteorological wind speed of 6 m/s it is unlikely to obtain satisfactory pressure difference measurements. At the last bin between 6 and 7 m/s, the OLS seems to obtain better values again (compared to the previous bin). However, this last bin needs to be treated with caution because it contains only one single measurement. All other bins include far more than one measurement and are therefore more reliable.

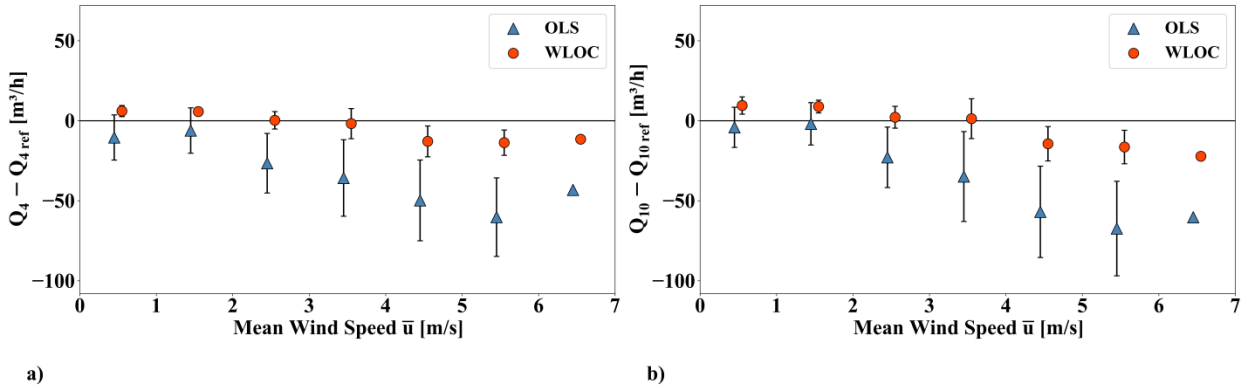

FIG. 8 Average relative airflow rate as a function of the mean wind speed at (a) 4 Pa and (b) 10 Pa pressure difference binned every 1 m/s of wind speed

Figure 9 shows the average relative ELAs at 4 (a) and 10 Pa (b) pressure difference. Here, the differences between the calculated values and the reference value increase much more with the mean wind speed for OLS. The vertical bars show the variability in ELA within each bin. In

contrast to the relative airflow rate, the error of predicted ELAs seems to increase with decreasing pressure. The error for extrapolation up to 4 Pa is in this specific configuration for OLS higher than for 10 Pa. The error for WLOC seems to remain more or less the same. Again, the last bin contains only one value.

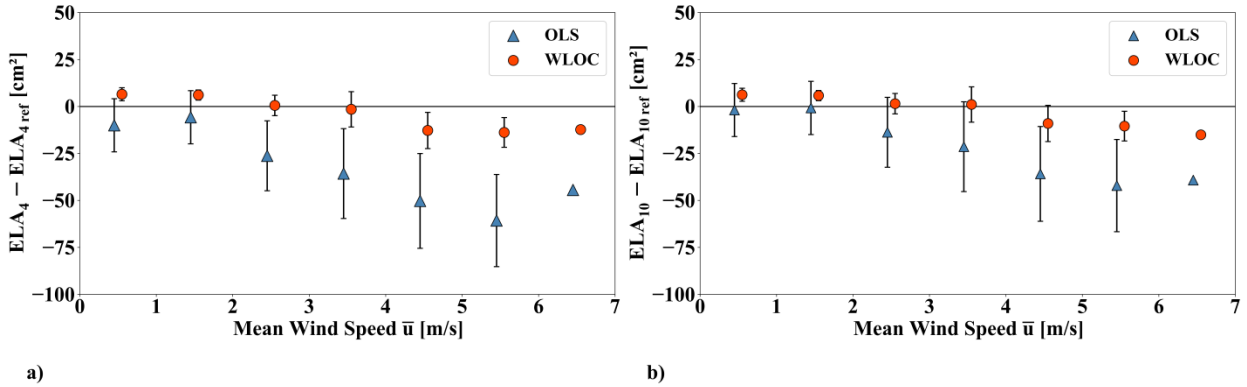

FIG. 9 Average relative equivalent leakage area as a function of the mean wind speed at (a) 4 Pa and (b) 10 Pa pressure difference binned every 1 m/s of wind speed

In general, Figures 8 and 9 show that OLS has much higher wind-induced biases, and these biases toughly increase with wind speed. Even though standards (e.g., [10]) allow fan pressurization measurements up to 6 m/s, these findings show that the extrapolation error of OLS is much higher in this range compared to WLOC.

4. Conclusion and Future Work

WLOC reduces the variances for pressure exponent *n* and flow coefficient *C*, typically by 32 % and 22 %, respectively, averaged over 7402 fan pressurization tests. Therefore, the use of this analysis technique is encouraged and should be adopted by building test standards. One caveat is that each pressure station needs to record the uncertainty (variance or standards

deviation) at each point in addition to the mean. Given modern test equipment and test automation, this should not be too much of a barrier. Work will be required with test equipment manufacturers to incorporate the recording of these data, together with the calculation procedures for WLOC.

5. NOMENCLATURE

Abbreviations

AHHRF	Alberta Home Research Facility
ELA	Equivalent Leakage Area
IWLS	Iterative Weighted Least Square
KDE	Kernel Density Estimation
OLS	Ordinary Least Square
PDF	Probability Density Function
WLOC	Weighted Line of Organic Correlation

Latin Symbols

C	Flow coefficient [$m^3/(h \cdot Pa^n)$]
C_D	Discharge coefficient [-]
$\widehat{f_h}(x_s)$	Density function which approximated the probability density function
N	Number of measurement points
n	Pressure exponent [-]
P	Pressure [Pa]
Q	Airflow [m^3/h]
u	Wind speed [m/s]

v_i	Weight of the x-value
w_i	Weight of the y-value
x_i	Measurement coordinate which corresponds to $\ln(\Delta P_i)$
x_s	Data samples
y_i	Measurement coordinate which corresponds to $\ln(Q_i)$

Greek Symbols

Δ	Difference
ρ	Density of air [kg/m³]
σ	Standard deviation

Subscripts

4	Evaluated at 4 Pa pressure difference
10	Evaluated at 10 Pa pressure difference
i	Single measurement point
ref	Reference point

6. ACKNOWLEDGMENTS

The presented work was embedded in a research project of the German Aerospace Center (DLR), which is funded by the German Ministry for Economic Affairs and Energy (grant number 03ET1405A) in cooperation with the Lawrence Berkeley National Laboratory (LBNL), CA, USA.

7. REFERENCES

[1] IEA - Global Alliance for Buildings and Construction. 2019 Global Status Report for

Buildings and Construction: Towards a zero-emission, efficient and resilient buildings and construction sector; 2019.

[2] Jokisalo J, Kurnitski J, Korpi M, Kalamees T, Vinha J. Building leakage, infiltration, and energy performance analyses for Finnish detached houses. Building and Environment 2009;44(2):377–87. https://doi.org/10.1016/j.buildenv.2008.03.014.

[3] Feijó-Muñoz J, Pardal C, Echarri V, Fernández-Agüera J, Assiego de Larriva R, Montesdeoca Calderín M et al. Energy impact of the air infiltration in residential buildings in the Mediterranean area of Spain and the Canary islands. Energy and Buildings 2019;188-189:226–38. https://doi.org/10.1016/j.enbuild.2019.02.023.

[4] Jones B, Das P, Chalabi Z, Davies M, Hamilton I, Lowe R et al. Assessing uncertainty in housing stock infiltration rates and associated heat loss: English and UK case studies. Building and Environment 2015;92:644–56. https://doi.org/10.1016/j.buildenv.2015.05.033.

[5] Chan WR, Joh J, Sherman MH. Analysis of air leakage measurements of US houses. Energy and Buildings 2013;66:616–25. https://doi.org/10.1016/j.enbuild.2013.07.047.

[6] Borsboom W, Kornaat W, van Beek P, Bink N-J, Lanooy T. Commission and performance contracting of ventilation systems in practice. Determination, analyses and consequences for practitioners and contractors. In: Proceedings of the 40th AIVC Conference; 2019.

[7] Hens H. Building Physics - Heat, Air and Moisture. Berlin, Germany: Ernst & Sohn Verlag für Architektur und technische Wissenschaften GmbH & Co. KG; 2012.

[8] TenWolde A. Ventilation, humidity and condensation in manufactured houses during winter. ASHRAE Transactions 1994;100(1):103–15.

[9] ASTM. E779-19 Test Method for Determining Air Leakage Rate by Fan Pressurization;91.140.30(E779 - 19). West Conshohocken, PA: ASTM International; 2019.

https://doi.org/10.1520/E0779-19.

[10] DIN. DIN EN ISO 9972:2018-12, Thermal performance of buildings - Determination of air permeability of buildings - Fan pressurization method. 12th ed;9972:2018(DIN EN ISO 9972:2018-12). Berlin: Beuth Verlag GmbH; 2018. https://doi.org/10.31030/3002630.

[11] CAN/CGSB. 149.10-2019 Determination of the Airtightness of Building Envelopes by the Fan Depressurization Method;91.120.10(149.10-2019). Gatineau: Canadian General Standards Board; 2019.

[12] Carrié FR, Leprince V. Model error due to steady wind in building pressurization tests. In: Proceedings of the 35th AIVC Conference; 2014.

[13] Carrié FR, Leprince V. Uncertainties in building pressurisation tests due to steady wind. Energy and Buildings 2016;116:656–65. https://doi.org/10.1016/j.enbuild.2016.01.029.

[14] Walker IS, Sherman MH, Joh J, Chan WR. Applying Large Datasets to Developing a Better Understanding of Air Leakage Measurement in Homes. International Journal of Ventilation 2013;11(4):323–38. https://doi.org/10.1080/14733315.2013.11683991.

[15] Ng LC, Musser A, Persily AK, Emmerich SJ. Multizone airflow models for calculating infiltration rates in commercial reference buildings. Energy and Buildings 2013;58:11–8. https://doi.org/10.1016/j.enbuild.2012.11.035.

[16] Vornanen-Winqvist C, Järvi K, Toomla S, Ahmed K, Andersson MA, Mikkola R et al. Ventilation Positive Pressure Intervention Effect on Indoor Air Quality in a School Building with Moisture Problems. Int J Environ Res Public Health 2018;15(2). https://doi.org/10.3390/ijerph15020230.

[17] Persily AK, Grot RA. Accuracy in Pressurization Data Analysis. ASHRAE Transactions 1985;91(2).

[18] Herrlin MK, Modera MP. Analysis of Errors for a Fan-Pressurization Technique for Measuring Inter-Zonal Air Leakage. In: Proceedings of the 9th AIVC Conference; 1988.

[19] Geissler A. Error estimation of blower door measurements by computer simulation. In: Proceedings of the 20th AIVC Conference; 1999.

[20] Sherman M, Palmiter L. Uncertainties in Fan Pressurization Measurements. In: Modera MP, editor. Airflow performance of building envelopes, components, and systems: Papers presented at a symposium held in Dallas/Ford Worth Airport, TX on 10 - 11 October 1993. Philadelphia, Pa.: ASTM; 1995, 266-266-18.

[21] Prignon M, Dawans A, Altomonte S, van Moeseke G. A method to quantify uncertainties in airtightness measurements: Zero-flow and envelope pressure. Energy and Buildings 2019;188-189:12–24. https://doi.org/10.1016/j.enbuild.2019.02.006.

[22] Carrié FR, Mélois A. Modelling building airtightness pressurisation tests with periodic wind and sharp-edged openings. Energy and Buildings 2020;208:109642. https://doi.org/10.1016/j.enbuild.2019.109642.

[23] Delmotte C, Laverge J. Interlaboratory tests for the determination of repeatability and reproducibility of buildings airtightness measurements. In: Proceedings of the 32nd AIVC Conference; 2011.

[24] Okuyama H, Onishi Y. Reconsideration of parameter estimation and reliability evaluation methods for building airtightness measurement using fan pressurization. Building and Environment 2012;47:373–84. https://doi.org/10.1016/j.buildenv.2011.06.027.

[25] Delmotte C. Airtightness of Buildings - Considerations regarding the Zero-Flow Pressure and the Weighted Line of Organic Correlation. In: Proceedings of the 38th AIVC Conference; 2017.

[26] Prignon M, Delmotte C, Dawans A, Altomonte S, van Moeseke G. On the impact of regression technique to airtightness measurements uncertainties. Energy and Buildings 2020;215:109919. https://doi.org/10.1016/j.enbuild.2020.109919.

[27] Prignon M, Dawans A, van Moeseke G. Uncertainties in airtightness measurements: regression methods and pressure sequences. In: Proceedings of the 39th AIVC Conference; 2018.

[28] Walker IS. Prediction of Ventilation, Heat Transfer and Moisture Transport in Attics [Dissertation]. Edmonton, Alberta: University of Alberta; 1993.

[29] Modera MP, Wilson DJ. The Effects of Wind on Residential Building Leakage Measurements. In: Sherman MH, editor. Air Change Rate and Airtightness in Buildings. West Conshohocken, PA: ASTM International; 1990, 132-145.

[30] Etheridge DW. The Rule of the Power Law - An Alternative View. Air Infiltration Review 1987;8(4):917.

[31] Dick JB. The Fundamentals of Natural Ventilation of Houses. Journal of the Institution of Heating and Ventilating Engineers 1950;18(179):123–34.

[32] Liddament MW. Power law rules - OK? Air Infiltration Review 1987;8(2):4–6.

[33] Sherman MH, Chan WR. Building Air Tightness: Research and Practice. In: Santamouris M, Wouters P, editors. Building Ventilation: The State of the Art. London: Routledge; 2006, p. 137–161.

[34] Walker IS, Wilson DJ, Sherman MH. A comparison of the power law to quadratic formulations for air infiltration calculations. Energy and Buildings 1998;27(3):293–9. https://doi.org/10.1016/S0378-7788(97)00047-9.

[35] Weisberg S. Applied Linear Regression. 3rd ed. Hoboken, New Jersey: John Wiley & Sons;

2005.

[36] Delmotte C. Airtightness of Buildings - Calculation of Combined Standard Uncertainty. In: Proceedings of the 34th AIVC Conference; 2013.

[37] Parzen E. On estimation of a probability density function and mode. The annals of mathematical statistics 1962;33(3):1065–76.

[38] Silverman BW. Density Estimation for Statistics and Data Analysis. 26th ed. Boca Raton, Florida: CRC press LLC; 1986.

[39] Węglarczyk S. Kernel density estimation and its application. ITM Web Conf. 2018;23(2):37. https://doi.org/10.1051/itmconf/20182300037.

[40] Sheather SJ. Density Estimation. Statistical Science 2004;19(4):588–97. https://doi.org/10.1214/088342304000000297.

[41] Lampe OD, Hauser H. Interactive visualization of streaming data with kernel density estimation. In: Proceedings of the IEEE Pacific Visualization Symposium; 2011, p. 171–178.